

## Bulk Polymerization of Vinyl Chloride

AHMED H. ABDEL-ALIM AND A. E. HAMIELEC, *Department of Chemical Engineering, McMaster University, Hamilton, Ontario, Canada*

### Synopsis

The bulk polymerization of vinyl chloride initiated by AIBN at temperature levels of 30°, 50°, and 70°C has been studied. Molecular weight averages and distribution (MWD) were measured by gel permeation chromatography. A model has been proposed which accurately predicts conversion to high levels and MWD. Molecular weight measurements show that transfer to monomer plays the important role in controlling molecular weight averages. Disproportionation is probably the dominant mode of termination.

### INTRODUCTION

Many workers have studied experimentally bulk polymerization of vinyl chloride.<sup>1-14</sup> A common observation was autocatalysis from the onset of the reaction. A review of these works is given by Talamini and Pegion.<sup>15</sup> Most of the models proposed to date fit experimental rates only up to relatively small conversions. An exception is the model recently proposed by Talamini,<sup>10,13</sup> which predicts rates of polymerization accurately up to about 70% conversion.

A comprehensive investigation of reaction parameters on molecular weight averages and distribution (MWD) has so far not been reported. This paper reports an experimental study of vinyl chloride bulk polymerization with special emphasis on molecular weight and MWD measurements. Also reported is the development of a model which applies to almost complete conversion. This model is similar to that of Talamini, with some modifications regarding the change in volume during polymerization as well as the consumption of initiator.

### THEORY

Talamini's model assumes a two-phase polymerization, in a monomer-rich and polymer-rich phase. The polymer is treated as a single component, with the concentration of monomer and polymer remaining constant during the polymerization. As reaction proceeds, the mass of polymer-rich phase grows while the monomer-rich phase diminishes. The initiator is assumed to have the same concentration in both phases. Experimental evidence indicates that the onset of two phases begins after less than 1% conversion and lasts until between 70% and 80% conversion,

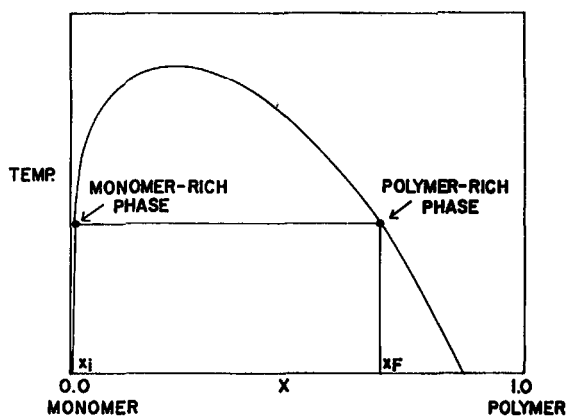


Fig. 1. Equilibrium binary diagram between pure monomer and pure polymer (suggested).

depending on the temperature. Talamini's model can be represented on a binary, two-phase equilibrium diagram shown in Figure 1.

### MODEL DEVELOPMENT

The present model assumes the presence of two phases in equilibrium, each of constant composition ( $x_i$  and  $x_f$  % of polymer, respectively), Figure 1.  $x_i$  is very small,<sup>13</sup> so it is taken as 0, that is, the monomer-rich phase contains only monomer.

A material balance for polymer gives

$$xM_T = x_fM_2 \quad (1)$$

$$\therefore M_2 = M_T \frac{x}{x_f} \quad (2)$$

$$\therefore M_1 = M_T \frac{x_f - x}{x_f} \quad (3)$$

The density of the mixture at conversion  $x$  is given by

$$\frac{1}{\rho} = \frac{x}{\rho_p} + \frac{1-x}{\rho_m} \quad (4)$$

from which the change of volume with conversion is given by

$$V = V_0(1 - Bx) \quad (5)$$

where

$$B = \frac{\rho_p - \rho_m}{\rho_p}$$

This relation was also used to calculate conversion by dilatometry. Since the concentration of monomer in the monomer-rich phase clearly is unit

mole fraction, it can be shown that monomer concentration in the polymer-rich phase is given by

$$[M_2] = \frac{\rho_2}{\rho_m} (1 - x_f) \text{ mole fraction} \quad (6)$$

$$[M_1] = 1.0 \text{ mole fraction} \quad (7)$$

where

$$\frac{1}{\rho_2} = \frac{x_f}{\rho_p} + \frac{1 - x_f}{\rho_m}$$

For unit volume of reaction mixture, total moles of monomer = moles monomer in monomer-rich phase + moles monomer in polymer-rich phase;

$$\therefore M_T \frac{dx}{dt} = R_{p_1} + R_{p_2}$$

$$R_{p_1} = R_1 M_T \frac{x_f - x}{x_f} \text{ moles/time} \quad (8)$$

$$R_{p_2} = R_2 M_T \frac{x}{x_f} (1 - x_f) \text{ moles/time} \quad (9)$$

where  $R_1$  and  $R_2$  are expressed in conversion/unit time;

$$\therefore \frac{dx}{dt} = R_1 \left( \frac{x_f - x}{x_f} \right) + R_2 x \left( \frac{1 - x_f}{x_f} \right)$$

The polymerization in the polymer-rich phase might be diffusion controlled, and we therefore set  $R_2 = PR_1$ , where  $P$  is a constant greater than unity, and

$$\frac{dx}{dt} = R_1(1 + Qx)$$

where

$$Q = \frac{P(1 - x_f) - 1}{x_f} \quad (10)$$

From the theory of homogeneous kinetics,

$$R = k_p \left( \frac{fk_d I}{k_t} \right)^{1/2} = kI^{1/2} \quad (11)$$

where

$$k = k_p (f \cdot k_d / k_t)^{1/2} \quad (12)$$

$$\therefore R_1 = k_1 I^{1/2}$$

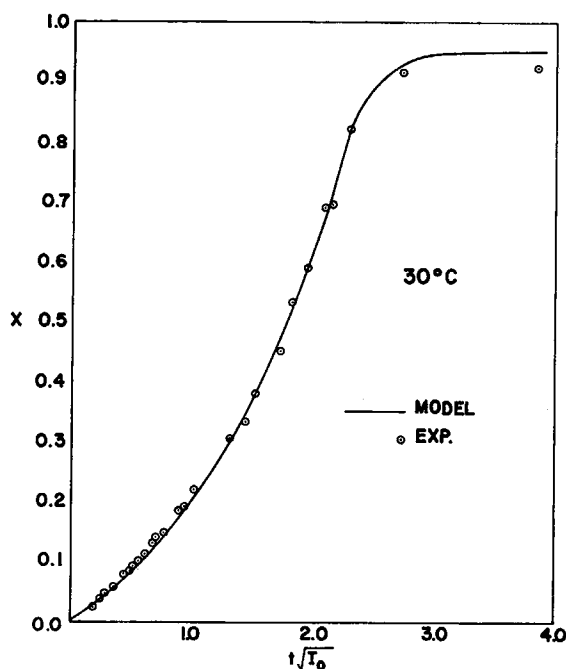


Fig. 2. Conversion curve at 30°C;  $x$  is conversion,  $t$  is reaction time in hr; and  $i_0$  is initial initiator concentration in g/g VC.

If we take into account the variation of the volume with conversion and the consumption of the initiator, then

$$I = I_0 \frac{\exp(-k_d \cdot t)}{(1 - Bx)}$$

$$\therefore \frac{dx}{dt} = \frac{1 + Qx}{\sqrt{1 - Bx}} \cdot k_1 I_0^{1/2} \exp\left(-\frac{k_d \cdot t}{2}\right). \quad (13)$$

Substituting  $x = 0$  in eq. (13) yields

$$\left(\frac{dx}{dt}\right)_0 = k_1 I_0^{1/2}.$$

This means that the constant  $k_1$  is simply the initial slope of the curve  $x$  versus  $t\sqrt{I_0}$ , Figures 2 and 3.

Equation (13) describes the system up to conversion of  $x_f$ ; it is easily solved analytically with the initial conditions  $x = x_i = 0$  at  $t = 0$ . However, the solution is more readily obtained when  $t$  is expressed as an explicit function of  $x$  rather than the reverse; it is given by

$$t = -\frac{2}{k_d} \ln(1 - H) \quad (14)$$

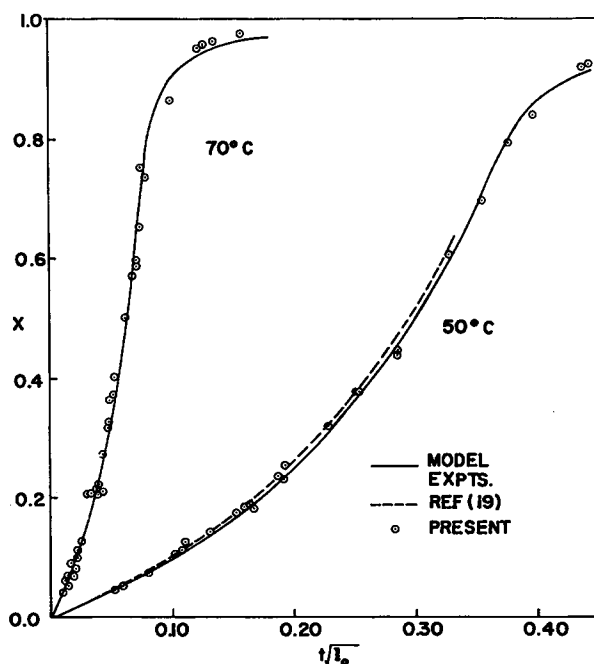


Fig. 3. Conversion curves at 50°C and 70°C; parameters same as Fig. 2; (—) suspension data from ref. (19).

where

$$H = \frac{k_a}{2k_t I_0^{1/2}} \left[ \frac{2}{Q} (\sqrt{1 - Bx} - 1) + \frac{\sqrt{Q + B}}{Q\sqrt{Q}} \ln \left( \frac{\sqrt{Q(1 - Bx)} - \sqrt{Q + B}}{\sqrt{Q} - \sqrt{Q + B}} \cdot \frac{\sqrt{Q(1 - Bx)} + \sqrt{Q + B}}{\sqrt{Q} + \sqrt{Q + B}} \right) \right]$$

Undoubtedly,  $k_t$  will continue to fall with conversion in the region  $x > x_f$ , and near the glass transition point  $k_p$  will approach zero and the polymerization will cease. Because the contribution of transfer to monomer is so much greater than termination by disproportionation<sup>16</sup> with respect to the polymer molecular weights, we can assume that  $k$  is proportional to the monomer concentration, with small error in the prediction of MWD and molecular weight averages. It is difficult to assess the error in the prediction of conversion because  $f$ ,  $k_t$ , and  $k_p$  will all fall with conversion; we have decided for our model to assume that the combined group  $k$  changes with  $(1 - x)$ , for  $x$  values greater than  $x_f$ .

It is assumed that the initiator concentrations are the same in both phases for the initiator under study. (However, for other initiators, we can assume a partition coefficient not equal to unity.) Diffusion control in the polymer-rich phase leads to a much lower  $k_t$  value, which gives rise to a higher  $k$  value; accordingly,

$$k_2 = P \cdot k_1 \quad (15)$$

$$\text{For } x > x_f: \quad \therefore k \propto (1 - x) \quad (16)$$

$$\therefore k = Pk_1 \frac{1 - x}{1 - x_f}$$

The rate of reaction can then be written as

$$-\frac{d[M]}{dt} = Pk_1 \left( \frac{1 - x}{1 - x_f} \right) I_0^{1/2} \frac{\exp\left(-\frac{k_d \cdot t}{2}\right)}{\sqrt{1 - Bx}} M_T(1 - x)$$

or

$$\frac{dx}{dt} = \frac{Pk_1}{1 - x_f} I_0^{1/2} \frac{(1 - x)^2}{\sqrt{1 - Bx}} \cdot \exp\left(-\frac{k_d \cdot t}{2}\right) \quad (17)$$

Again, eq. (17) is easily solved analytically, and the solution is better expressed as  $t$  explicitly in  $x$ ,

$$t = -\frac{2}{k_d} \ln(1 - HH) + t_f \quad (18)$$

where  $t_f$  is the time to reach  $x_f$ , and

$$HH = \frac{(1 - x_f)k_d}{2Pk_1 I_0^{1/2}} \left\{ \frac{\sqrt{1 - Bx}}{1 - x} - \frac{\sqrt{1 - Bx_f}}{1 - x_f} \right. \\ \left. + \frac{B}{2\sqrt{1 - B}} \ln \frac{\left( \frac{\sqrt{1 - x} - \sqrt{1 - B}}{\sqrt{1 - x_f} - \sqrt{1 - B}} \right)}{\left( \frac{\sqrt{1 - x} + \sqrt{1 - B}}{\sqrt{1 - x_f} + \sqrt{1 - B}} \right)} \right\}$$

## MOLECULAR WEIGHT AVERAGES AND DISTRIBUTION

The measured molecular weights had a polydispersity of 2 or slightly higher. If polymer produced in each phase has a polydispersity of 2, the polydispersity of the mixed polymer will be equal to or greater than 2.

From homogeneous kinetics, it can be shown that, for termination by disproportionation and transfer to monomer,

$$W_r = \tau^2 r \cdot \exp(-\tau r) \quad (19)$$

where  $\tau$  is given by

$$\tau = C_M + \frac{(fk_d k_t)^{1/2} I^{1/2}}{k_p [M]} \quad (20)$$

Substituting from eq. (12) into eq. (20),

$$\tau = C_M + \frac{fk_d I^{1/2}}{k[M]} \quad (21)$$

The MWD of the total polymer mixture is obtained from

$$W_r = m_1 \cdot W_{r_1} + m_2 \cdot W_{r_2} \quad (22)$$

It is assumed that  $C_M$  is the same in both phases; this assumption is confirmed by the work of Talamini<sup>16</sup> and Danusso<sup>17</sup> who obtained almost the same value of  $C_M$  by applying the Mayo equation to data from solution polymerization (homogeneous) and bulk polymerization (heterogeneous), respectively.

From equations (6), (7), and (21),

$$\tau_1 = C_M + \frac{fk_d I_0^{1/2}}{k_1 \sqrt{1 - Bx}} \cdot \exp\left(-\frac{k_d t}{2}\right) \quad (23)$$

$$\tau_2 = C_M + \frac{fk_d \rho_m I_0^{1/2}}{pk_1 \rho_2 (1 - x_f) \sqrt{1 - Bx}} \cdot \exp\left(-\frac{k_d t}{2}\right) \quad (24)$$

$$m_1 = \frac{mp_1}{M_{rx}}$$

$$mp_1 = \int_0^t R_{p_1} dt = \frac{M_T}{Q^2 x_f} [(Qx_f + 1) \ln(1 + Qx) - Qx]$$

$$m_1 = \frac{(Qx_f + 1) \ln(1 + Qx) - Qx}{Q^2 x_f} \quad (25)$$

Similarly,

$$m_2 = \frac{mp_2}{M_{rx}}$$

$$mp_2 = \int_0^t R_{p_2} dt$$

$$m_2 = \frac{P(1 - x_f)[Qx - \ln(1 + Qx)]}{Q^2 x_f} \quad (26)$$

For the MWD of eq. (22), it can be shown that

$$\int_0^{\infty} \frac{W_r}{r} dr = m_1\tau_1 + m_2\tau_2$$

$$\int_0^{\infty} W_r dr = 1.0$$

$$\int_0^{\infty} rW_r dr = 2 \left( \frac{m_1}{\tau_1} + \frac{m_2}{\tau_2} \right)$$

$$\therefore \bar{r}_n = \frac{1}{m_1\tau_1 + m_2\tau_2} \quad (27)$$

$$\bar{r}_w = \frac{2m_1}{\tau_1} + \frac{2m_2}{\tau_2} \quad (28)$$

$$\bar{r}_w/\bar{r}_n = \left( \frac{2m_1}{\tau_1} + \frac{2m_2}{\tau_2} \right) (m_1\tau_1 + m_2\tau_2). \quad (29)$$

This polydispersity will be equal to or greater than 2. For conversions higher than  $x_f$ , we assumed before that

$$k \propto (1 - x).$$

With small error we can write

$$\frac{fk_d}{k} \propto k$$

or

$$\frac{fk_d}{k[M]} \simeq \text{constant} \quad \text{for } x > x_f$$

or

$$\therefore \frac{fk_d}{k[M]} (\text{for } x > x_f) = \frac{fk_d}{Pk_1[M]} (\text{at } x = x_f). \quad (30)$$

From eq. (30) we can see that  $\tau$  of the polymer produced after  $x_f$  will practically be the same as that which was produced in the polymer-rich phase. So, after  $x_f$  we still can differentiate between two kinds of polymers only, the one that was produced in the monomer-rich phase and the one that was produced in the polymer-rich phase plus that polymer produced after  $x_f$ .

It can be shown that after  $x_f$

$$m_1 = (m_1)_{x=x_f} \cdot \frac{x_f}{x} \quad (31)$$

$$m_2 = \frac{p(1-x_f)[Qx_f - \ln(1+Qx_f)] + Q^2x_f(x-x_f)}{Q^2xx_f} \quad (32)$$

Equations (31) and (32) with eqs. (22), (23), (24), (27), (28), and (29) could be used to obtain the MWD and molecular weight averages.



## EXPERIMENTAL

**Operating Conditions.** Polymerization temperature: 30°, 50°, and 70°C controlled to  $\pm 0.1^\circ\text{C}$ . Initiator (AIBN) concentration: 0.3 to 3.2 wt-%.

**Polymerization Procedure.** Bulk polymerization in glass ampoules having 10 mm O.D. and 8 mm I.D. Conversions were determined gravimetrically. For conversions below about 20%, dilatometry was employed; dilatometers were about 6 ml in capacity, with a capillary of 2 mm I.D. These ampoules and capillary gave negligible temperature rise during polymerization.

**MWD and Averages.** Waters Model 200 GPC was used; THF was used as a solvent, temp. 30°C, flow rate 3 ml/min. A train of nine columns was used to give high resolution; these columns were: Bio-glas, 2500/1500 Å; CPG 10, 2000/1250 Å; CPG 10, 2000/1250 Å; CPG 10, 2000 Å; CPG 10, 700 Å; Styragel,  $10^4$  Å; Styragel, 800 Å; Styragel, 350/100 Å; Styragel, 350/100 Å. This column combination gave very good resolution, and correction for axial dispersion was negligible. A universal calibration curve was first obtained using polystyrene standards; then a PVC calibration curve was obtained from it, using the hydrodynamic volume concept. A search was employed to get the best values of Mark-Houwink constants to fit the PVC standards. This method was suggested by Provder.<sup>25</sup> The Mark-Houwink values used were  $K = 1.48 \times 10^{-4}$  and  $\epsilon = 0.768$ . A nonlinear calibration curve was obtained in the form

$$\text{mol. wt.} = D_1 \exp(-D_2v - D_3v^2 - D_4v^3).$$

From the reproducibility study performed for this work, the confidence limits at a confidence level of 95% are given in Table I for the measured quantities.

TABLE I  
Reproducibility of Measured Quantities

Quantity measured	Confidence limits (95% conf. level)	
	mean	
Conversion $x$	$\pm 2.42\%$	
$\bar{M}_n$	$\pm 6.96\%$	
$\bar{M}_w$	$\pm 5.75\%$	
$\bar{M}_w/\bar{M}_n$	$\pm 1.44\%$	

## RESULTS AND DISCUSSIONS

It is well established from previous work<sup>13,14</sup> that conversion curves completely overlap when they are plotted as  $x$  versus  $t\sqrt{I_0}$  instead of  $x$  versus  $t$  (time). This was also observed in the present work. The solution of the proposed kinetic equations shows that the parameter  $t\sqrt{I_0}$  assumes a constant value at a certain conversion and temperature, irrespective of

TABLE II  
 Parameters of Present Model\*

Temp., °C	$x_f$	$Q$	$k_1, \frac{1}{\text{hr (mole-%)^{1/2}}}$	$P$	$C_M \times 10^3$
30	0.80	4.5	0.23	23.0	0.63
50	0.77	5.5	1.25	22.7	1.10
70	0.72	5.1	6.21	16.7	5.71

\*  $C_M = 5.78 \exp(-2768.1/T)$ ;  $k_1 = 3.54 \times 10^{11} \exp(-8505.5/T)$ .

TABLE III

Values of $k_p^2/k_t$	
Temp., °C	$(k_p^2/k_t) \times 10^{-2}$
30	1.89
50	2.41
70	3.61

• In units of  $\text{hr}^{-1} (\text{mole } \%)^{-1}$ .

the value of  $I_0$  in the working region. Accordingly, this type of plot was used in this work.

Figures (2) and (3) show the conversion curves for the three temperature levels 30°, 50°, and 70°C. The theoretical curves from eqs. (14) and (18), using the values of  $Q$ ,  $x_f$ , and  $k_1$  given in Table II, are also shown in the figures. Agreement between experimental curves and model predictions is satisfactory. At 30°C for conversions greater than 90%, the experimental points show lower conversion values than the model. This does not appear in the 50°C and 70° curves. The choice of  $Q$  dictates the fit of the conversion data, and it appears that our single parameter model is inadequate over the entire conversion range at 30°C. Agreement at 50°C and 70°C, temperatures which are often used commercially, is much better. Experimental data of Farber and Koral<sup>19</sup> for suspension polymerization at 50°C are also compared in Figure 3; the good agreement suggests that the same kinetic model would apply as well for suspension polymerization.

The values of the parameters used in the model are listed in Table II. These values were obtained as follows:

$k_1$ . As shown from eq. (13), the value of  $k_1$  at each temperature represents the initial slope of the curve  $x$  versus  $t \sqrt{I_0}$  for this temperature. In fact, eq. (13) has the form

$$\frac{dx}{dt} = \left( \frac{dx}{dt} \right)_0 \cdot F(x,t).$$

Here,  $F(x,t)$  represents an accelerating function. From the values of  $k_1$  we can obtain values for  $k_p^2/k_t$  in the monomer-rich phase at each temperature, using  $f = 1.0$  and the appropriate  $k_d$  value. This is shown in Table III. However, although we can get the value of  $k$  in the polymer-rich

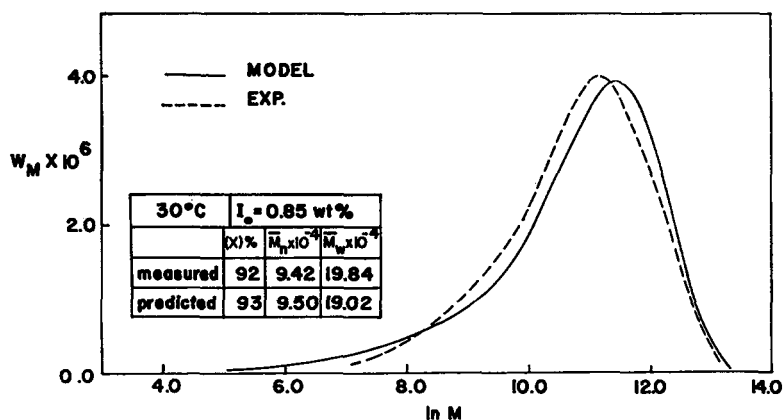


Fig. 4. Experimental and theoretical MWD at 30°C.

phase, we still have to know the value of  $f$  in this phase in order to calculate  $k_p^2/k_t$ . The assumption of  $f = 1$  in both phases does not lead to serious errors when calculating molecular weights because of strong transfer to monomer; this assumption is questionable, however, when getting a value for  $k_p^2/k_t$  in the polymer-rich phase.

$x_f$ . This represents the highest conversion below which the two-phase model fits the experimental data. It is obtained by comparing the experimental curves with eq. (14). As shown in Table II,  $x_f$  increases with decrease in temperature, which is expected as  $x_f$  represents the composition of the polymer-rich phase. As temperature decreases, the solubility of monomer in polymer decreases, giving rise to a polymer-rich phase of higher polymer content. In fact, a detailed study of polymerization at different temperatures could lead to the construction of the equilibrium diagram shown in Figure 1.

$k_d$ . As a function of temperature, this was obtained from the literature<sup>17</sup> as

$$k_d = 3.79 \times 10^{13} \exp(-15460/T) \text{ hr}^{-1}.$$

$C_M$ . Obtained from the literature,<sup>16,20</sup> and slightly modified to fit the experimental data:

$$C_M = 5.78 \exp(-2768.1/T).$$

$Q$ . This is the only parameter that was searched for; the values chosen were those to give the best agreement. Values of  $p$  are obtained from  $Q$  using eq. (10). Table II also shows a decrease in  $p$  with increasing temperature. The same discussion of variation of  $x_f$  with temperature holds for the effect of temperature on  $P$ .

Figures 4, 5, and 6 show a comparison between the measured and predicted MWD at 30°, 50°, and 70°C, respectively. The agreement between the two curves supports the assumption that termination by com-

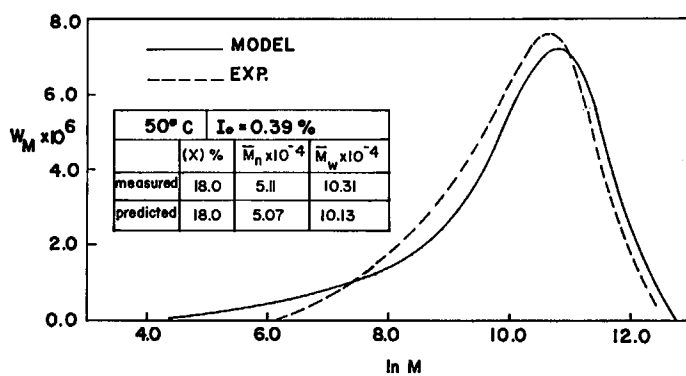


Fig. 5. Experimental and theoretical MWD at 50°C.

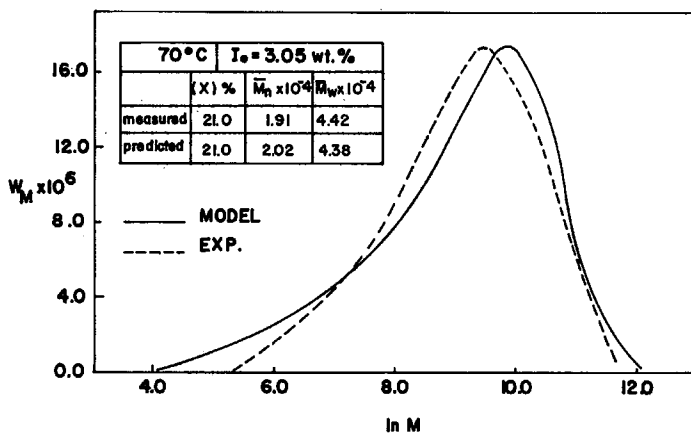
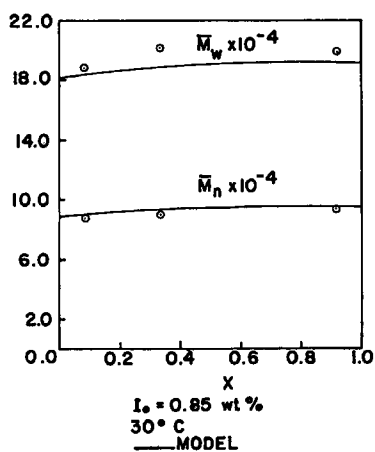


Fig. 6. Experimental and theoretical MWD at 70°C.

Fig. 7. Effect of conversion on  $\bar{M}_w$  and  $\bar{M}_n$  at 30°C.

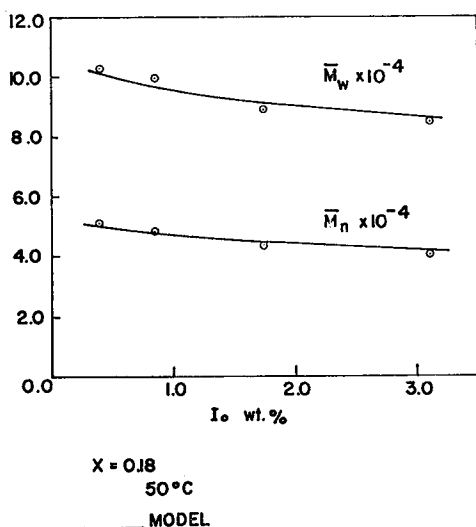


Fig. 8. Effect of initiator concentration on  $\bar{M}_w$  and  $\bar{M}_n$  at  $50^\circ\text{C}$ .

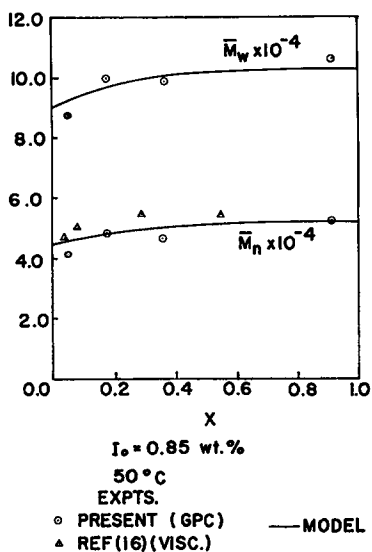


Fig. 9. Effect of conversion on  $\bar{M}_w$  and  $\bar{M}_n$  at  $50^\circ\text{C}$ .

bination and disproportionation is much smaller than that of transfer to monomer. It is noted that the measured DMWD is shifted slightly to lower molecular weights; the reason for this could be small uncorrected axial dispersion effects, such as skewing in gel permeation chromatography.

In Figures 7 to 11, experimental and predicted molecular weight averages are shown. A slight increase in  $\bar{M}_n$  and  $\bar{M}_w$  is noted with conversion; it is more significant below about 20% conversion as was noticed by Danusso<sup>17</sup> at  $50^\circ\text{C}$ . Also, as expected, there is a slight decrease in  $\bar{M}_n$  and

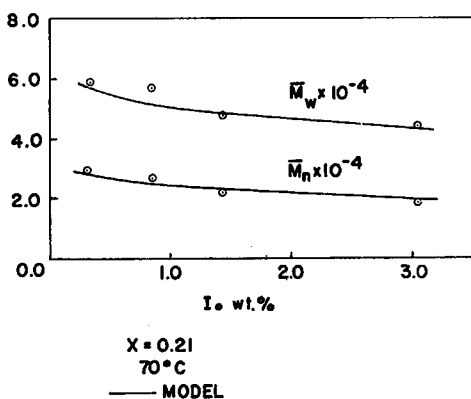


Fig. 10. Effect of initiator concentration on  $\bar{M}_w$  and  $\bar{M}_n$  at  $70^\circ\text{C}$ .

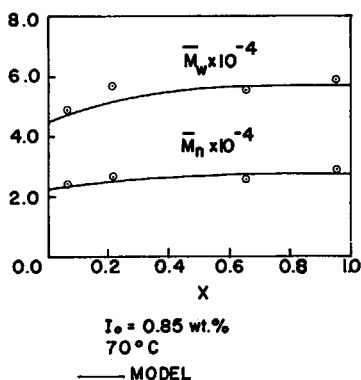


Fig. 11. Effect of conversion on  $\bar{M}_w$  and  $\bar{M}_n$  at  $70^\circ\text{C}$ .

$\bar{M}_w$  with increasing initiator concentration. This apparent independency of molecular weight averages on conversion or initiator concentration is probably the result of the strong transfer to monomer.<sup>3,9,16</sup>

Figure 9 shows also the results of Vidotto<sup>16</sup> for  $\bar{M}_n$  values at  $50^\circ\text{C}$ , using lauroyl peroxide as an initiator (0.89 wt-%) measured by viscometry. These values are slightly higher than our values measured by GPC.

It was noticed that the variation of  $\bar{M}_n$  and  $\bar{M}_w$  with conversion is more pronounced at higher temperatures (Figs. 7, 9, and 11). The reason for this could be that at lower temperatures  $C_M$  is much higher than  $fk_d I^{1/2}/k[M]$ , which is a function of conversion. Accordingly,  $\tau$  will not vary much with conversion, since  $C_M$  is assumed the same in both phases; then  $\tau_1$  and  $\tau_2$  will be close to each other and not varying much with conversion, hence, molecular weight averages will not vary much with conversion. At higher temperatures, the relative importance of  $fk_d I^{1/2}/k[M]$  increases, and hence  $\tau_1$  will be more different than  $\tau_2$  giving rise to more variation of molecular weight averages with conversion.

TABLE IV  
Predictions of Polydispersity—Present Model<sup>a</sup>

Conversion $x$	$\bar{M}_w/\bar{M}_n$		
	30°C	50°C	70°C
0.00	2.0000	2.0000	2.0000
0.10	2.0028	2.0151	2.0492
0.20	2.0039	2.0199	2.0651
0.30	2.0043	2.0215	2.0699
0.40	2.0045	2.0217	2.0702
0.50	2.0045	2.0213	2.0686
0.60	2.0044	2.0207	2.0661
0.70	2.0043	2.0200	2.0632
0.80	2.0042	2.0192	2.0609
0.90	2.0040	2.0185	2.0579
0.99	2.0039	2.0171	2.0416

<sup>a</sup>  $I_0 = 0.85$  wt-%.

Table IV shows the predicted variation of the polydispersity with conversion at 30°, 50°, and 70°C. An increase in the polydispersity is noticed with increasing temperature at the same conversion level; this is in agreement with the above explanation.

If an Arrhenius plot is made for the obtained value of  $k_t$ , we can get the apparent activation energy of the reaction. This was found to be 16.9 kcal/mole. On the other hand, this activation energy could be calculated from the equation

$$E_a = E_i/2 + E_p - E_t/2$$

where  $E_a$ ,  $E_i$ ,  $E_p$ , and  $E_t$  are the apparent activation energy, the overall initiation, propagation, and termination activation energies, respectively. Danusso and Sianesi<sup>26</sup> reported a value for  $(E_p - E_t/2)$  of 1.5 kcal/mole, using the literature value of 30.7 kcal/mole for  $E_i$ ; a value of 16.85 kcal/mole was found for  $E_a$ , which is in excellent agreement with our experimental value.

### Nomenclature

$C_M$	monomer transfer constant
$f$	initiator efficiency
$I$	initiator concentration
$K$	Mark-Houwink constant
$k$	kinetic parameter, eq. (12)
$k_p$	propagation rate constant
$k_d$	initiator decomposition rate constant
$k_t$	termination rate constant
$M$	molecular weight
$M_T$	total mass of the system
$M_1$	mass of monomer-rich phase

$M_2$	mass of polymer-rich phase
$\bar{M}_n$	number-average molecular weight
$\bar{M}_w$	weight-average molecular weight
[M]	monomer concentration
$m_1$	mass fraction of polymer produced in monomer-rich phase
$m_2$	mass fraction of polymer produced in polymer-rich phase
$mp_1$	mass of polymer produced in monomer-rich phase
$mp_2$	mass of polymer produced in polymer-rich phase
$P, Q$	constants, eq. (10)
$r$	chain length
$R$	rate of polymerization as per cent conversion per unit time
$R_p$	rate of polymerization as moles (or mass) per unit time per unit volume
$\bar{r}_n$	number-average chain length
$\bar{r}_w$	weight-average chain length
$\bar{r}_w/\bar{r}_n$	polydispersity
$t$	reaction time
$T$	absolute temperature
$V$	volume
$v$	elution counts (volume)
$W_r$	weight fraction of polymer of chain length $r$
$W_m$	weight fraction of polymer of molecular weight $M$
$x$	conversion

#### Greek Symbols

$\rho$	density
$\epsilon$	Mark-Houwink constant
$\tau$	kinetic parameter, eq. (20)

#### Subscripts

$i, 1$	refers to monomer-rich phase
$f, 2$	refers to polymer-rich phase
$p$	refers to polymer
$m$	refers to monomer
0	refers to initial conditions ( $t = 0$ )

The authors are indebted to Imperial Oil Ltd., Canada, for financial support of this research project.

#### References

1. J. Prat, *M. Mem. Serv. Chim. Etat*, **32**, 319 (1946).
2. E. Jenckel, H. Eckmans, and H. Rumbac, *Makromol. Chem.*, **4**, 15 (1949).
3. W. J. Bengough and R. G. W. Norrish, *Proc. Roy. Soc. (London)*, **A220**, 301 (1950).
4. J. W. Breitenbach and A. Schindler, *Mh. Chem.*, **80**, 429 (1949); **86**, 437 (1955); *J. Polym. Sci.*, **18**, 435 (1955).
5. J. Arlman and W. M. Wagner, *J. Polym. Sci.*, **9**, 581 (1951).
6. F. Danusso and G. Perugini, *Chim. Ind. (Milan)*, **35**, 881 (1953).



7. A. Schindler and J. W. Breitenbach, *Ric. Sci., Suppl.*, **25**, 34 (1955).
8. M. Magat, *J. Polym. Sci.*, **16**, 491 (1955).
9. H. S. Mickley, A. S. Michaels, and A. L. Moore, *J. Polym. Sci.*, **60**, 121 (1962).
10. G. Talamini, G. Vidotto, *Makromol. Chem.*, **50**, 129 (1961); **53**, 21 (1962).
11. G. Talamini, *J. Polym. Sci. A2*, **4**, 535 (1966).
12. M. Ryska, C. M. Kolinsky, and D. Lim, *J. Polym. Sci.*, **C16**, 621 (1967).
13. A. Crosato-Arnaldi, P. Gasparini, and G. Talamini, *Makromol. Chem.*, **117**, 140 (1968).
14. J. D. Cotman, M. F. Gonzales, and G. G. Claver, *J. Polym. Sci. A1*, **5**, 1137 (1967).
15. G. Talamini and E. Peggion, in *Vinyl Polymerization*, Vol. I, G. Ham, Marcel Dekker, New York, 1967, Chap. 5.
16. G. Vidotto, A. Crosato-Arnaldi, and G. Talamini, *Makromol. Chem.*, **114**, 217 (1968).
17. F. Danusso, G. Pajaro, and D. Sianesi, *Chim. Ind. (Milan)*, **41**, 1170 (1959).
18. F. Danusso and G. Perugini, *Chim. Ind. (Milan)*, **35**, 881 (1953).
19. E. Farber and M. Koral, *Soc. Plast. Eng. Tech. Papers*, **13**, 398 (1967).
20. J. Brandup and E. H. Immergut, Eds., *Polymer Handbook*, Interscience, New York, 1966, II, 77.
21. Z. Mencik and J. Lanikova, *Coll. Czech. Chem. Commun.*, **21**, 257 (1956).
22. A. Crugnola and F. Danusso, *Polym. Letters*, **6**, 535 (1968).
23. P. Kratochvil, M. Bohdanecky, K. Solc, M. Kolinsky, M. Ryska, and D. Lim, *J. Polym. Sci. C*, **23**, 9 (1968).
24. J. Lyngaae-Jorgensen, *J. Chrom. Sci.*, **9**, 331 (1971).
25. T. Provder and E. M. Rosen, ACS Symposium on GPC, Houston, Texas, February 1970.
26. F. Danusso and D. Sianesi, *Chim. Ind. (Milan)*, **37**, 695 (1955).

Received September 13, 1971

Revised October 26, 1971